Lawrence Berkeley National Laboratory
Recent Work

Title
DENSIFICATION MECHANISMS IN HOT-PRESSING MAGNESIA WITH A FUGITIVE LIQUID

Permalink
https://escholarship.org/uc/item/2p25t29b

Authors
Hart, Patrick E.
Atkin, Robert B.
Pask, Joseph A.

Publication Date
1968-07-01

UCRL-18279

ey. 2

University of California

Ernest O. Lawrence Radiation Laboratory

DENSIFICATION MECHANISMS IN HOT-PRESSING
MAGNESIA WITH A FUGITIVE LIQUID

Patrick E. Hart, Robert B. Atkin and Joseph A. Pask

July 1968

Berkeley, California

UCRL - 18279 ey. 2

DISCLAIMER

To be submitted to
    J. Am. Ceram. Soc.

UNIVERSITY OF CALIFORNIA

Lawrence Radiation Laboratory
Berkeley, California

AEC Contract No. W-7405-eng-48

DENSIFICATION MECHANISMS IN HOT-PRESSING
MAGNESIA WITH A FUGITIVE LIQUID

Patrick E. Hart, Robert B. Atkin and Joseph A. Pask

July 1968

DENSIFICATION MECHANISMS IN HOT-PRESSING
MAGNESIA WITH A FUGITIVE LIQUID

Patrick E. Hart,[*] Robert B. Atkin and Joseph A. Pask

Inorganic Materials Research Division, Lawrence Radiation Laboratory,
and Department of Mineral Technology, College of Engineering,
University of California, Berkeley, California

July 1968

ABSTRACT

The densification of MgO with LiF additions occurs in three stages.
During hot pressing an adherent LiF-rich liquid film on MgO particles
provides lubrication for the rearrangement stage. Later, pressure-flow
enhanced liquid phase sintering is the dominant densification mechanism.
The kinetics of this stage are controlled by flow of the liquid film
as indicated by a density-$(time)^{-2/5}$ relationship which corresponds to
a densification rate-$(porosity)^{7/2}$ dependence. During the annealing
stage the remaining liquid film is vaporized resulting in fully trans-
parent polycrystalline MgO.

I. INTRODUCTION

Rice[1] first reported the effect of LiF additives on pressure sin-
tering of MgO and outlined processing procedures leading to transparent
specimens. A number of studies since then have made an effort to deter-
mine the densification mechanisms and optimum processing parameters.

Benecke et al.[2] proposed two mechanisms for the densification of
this system. On the basis of an observed particle size effect, plastic
deformation was suggested as a possible mechanism during early densifica-
tion. A diffusional grain boundary creep process occurring in an
activated surface layer on the MgO particles was suggested as a second
mechanism. Liquid phase sintering was rejected because densification
occurred below 848°C, the LiF melting point, and no discontinuity was
observed in the compaction behavior of specimens at this temperature
during heating at a constant rate and constant load. Stress enhanced
bulk diffusion was rejected because of unrealistically high diffusion
coefficients calculated using the Nabarro-Herring[3] relationship.

Rhodes et al.[4] proposed two mechanisms: (1) above the melting
point of LiF, a pressure-enhanced liquid phase sintering mechanism, and
(2) below the melting point, pressure-enhanced diffusion through a grain
boundary phase. X-ray lattice parameter studies performed on specimens
pressure sintered at 820°C indicated that Mg^{2+} and possible 0^{2-} were
soluble in the LiF lattice while Li^+ and F^- were both soluble in the
MgO lattice.

Carnall[5] has reported that kinetic data for pressure sintering of
the LiF-MgO system agrees with the liquid phase sintering model developed
by Kingery.[6] LiF was found effective in the removal of surface hydroxyl

and carbonate impurities from MgO.

Miles et al.[7] carried on extensive studies relative to the development of optimum fabrication processing parameters in the densification of MgO with a LiF additive.

Work of Vasilos and Spriggs[8] indicates that pressure sintering of MgO between 1100 and 1700°C is controlled by pressure enhanced diffusion. An activation energy of 78 kcal/mole for densification was calculated on the basis of the Nabarro-Herring[3] creep equation, and 95 kcal/mole using the Coble[9] sintering equation. The absolute values of diffusion coefficients calculated using both models were in good agreement with each other;[*] however, they were greater than those measured in self-diffusion and in unpublished pressureless sintering studies.

Brown[11] calculated an activation energy of 27 kcal/mole for pressureless sintering of high purity MgO between 1300 and 1500°C. Activation energies of 18 and 26 kcal/mole were measured for compacts containing 0.01 and 0.1% vanadium, respectively. These low activation energies, compared to self-diffusion values,[**] suggested grain boundary diffusion as the controlling densification mechanism.

Eastman and Cutler[14] found activation energies of 80 kcal/mole for the sintering of MgO in water vapor at pressures below 5 mm and 48 kcal/mole at pressures above 5 mm.

The objective of this work was to determine the kinetics and mechanisms controlling the fabrication of transparent polycrystalline

----

* Using the corrected sintering model reported by Coble and Gupta.[10]
** 79.0 kcal/mole for magnesium in MgO (Lindner and Parfitt).[12]
   62.4 kcal/mole for oxygen in MgO (Oishi and Kingery).[13]

MgO by pressure sintering (hot pressing) and subsequent annealing of LiF-MgO compacts.

II. EXPERIMENTAL PROCEDURE

A. Equipment and Materials

Pressure sintering was performed in reactor grade graphite dies (1 1/2 inches i.d.) and heated in a molybdenum-wound vacuum furnace. Temperature was measured with a Pt-Pt 10 Rh thermocouple inserted in the die body. Pressure was applied with a hydraulic ram and pump; specimen compaction was continuously monitored using a linear displacement transducer.

Baker and Adamson reagent grade MgO (Lot No. Y011--see Table I for characterization) was used for all specimens. Lithium fluoride was -125 mesh powder ground from single crystals prepared by Scott and Pask[15] using the Bridgman normal freezing method. The use of reagent grade LiF resulted in specimens of reduced optical quality.

B. Specimen Preparation

Thirty grams of MgO powder and the appropriate amount of LiF were mixed together in isopropyl alcohol and dried over night at 80°C. Batches were precompressed in the dies* at 1000 psi. The following heating schedule was begun after a vacuum of 10^{-4} torr was reached: 25°/ hour to 450°C then 500°C/hour to the pressing temperature. Pressure was normally applied when the specimen reached the desired temperature and released when the furnace began to cool. The range of pressing parameters is given in Table II. Specimens were removed from the die when

---

* Dies were presaturated with LiF; plunger faces were polished after each pressing to aid specimen removal and reduce graphite contamination.

the furnace had cooled to room temperature. Annealing of specimens was carried out in air and a vacuum at a heating rate of 60°C/hour up to temperatures of 1300°C.

Table II. Range of Pressing Parameters Employed

Variable	Range
Temperature	600-1300°C[*]
Pressure	1250-5250 psi
Pressing time	30-300 min
Initial LiF content	0.5-10 wt %

C. Specimen Evaluations

Densities were determined using a displacement technique. Absolute ethyl alcohol was selected as the displacement media.

Measurement of lithium content of hot pressed specimens was performed using flame spectro-photometric analysis. Lithium content of annealed specimens was below the limit of detectability. Accuracy of reported values is ± 10%.

Lattice parameters of hot-pressed specimens were determined using a Norelco diffractometer equipped with a crystal monochrometer. Spacings were corrected to 25°C using Skinner's expansion data.[16] Calculated lattice parameters for diffraction peaks were plotted against $\sin^2\theta$ and were extrapolated to $\sin^2\theta$ equal one.

---

* Samples pressed at temperatures below 670° and above 1100°C had open porosity after being held at temperature for 5 hours.

III. RESULTS

A. Densification

1. General Observations. Magnesium oxide compacts containing LiF additions densified while being heated to fabrication temperatures; subsequent load application resulted in flow of material out to the die walls. For example, a compact containing 3 wt% LiF that had been pre-compacted to a density of 54%* sintered to a density of 84% when heated to 900°C. On application of a stress of 2250 psi at 900°C, the initial compaction rate was about one in/hour. Some pre-sintering was observed in compacts at temperatures as low as 600°C.

When pressure was applied at room temperature, compacts showed a slight increase in density at about 325°C. Rapid densification started at temperatures between 550 and 600°C. Densification rates gradually decreased between 800 and 900°C approaching zero at about 1000°C. Discontinuities in compact length change during densification were not observed. Only the slight increase in density at about 325°C was observed on heating the compacts in the absence of LiF.[2]

An attempt was made to analyze compaction data in terms of the relationships derived for liquid phase sintering. Densification in such systems is considered by Kingery[6] to take place in three steps: an initial rearrangement step in which compact fractional shrinkage, $\frac{\Delta L}{L_0}$, is proportional to t^{1+y} where $(1+y)>1$; a solution-precipitation step where $\frac{\Delta L}{L_0} \propto t^{1/3}$; and a final coalescence step where $\frac{\Delta L}{L_0}$ approaches a constant value. A plot of $\log \frac{\Delta L}{L_0}$ vs log t for compacts containing 3% LiF

---

* Where densities are reported in percentages, the value is relative to the X-ray density of 3.583 gm/cm^3.

under a load of 2250 psi at 900°C showed no linear behavior. Slopes varied continuously between 0.5 and 0.1 for times greater than 5 minues after load application.

In order to present compaction data on a relative basis, specimen apparent densities during compaction were calculated from compact length change during densification, final sample length and density. In this calculation constant compact weight and composition during densification were assumed. An attempt was made to analyze the final hot-pressing stage using equations derived by Rossi and Fulrath[17] and by Fryer[18] for vacancy controlled diffusion processes. Calculated densities did not follow predicted porosity dependencies.

For a number of compacts, however, in the later stages of hot pressing the log of the densification rate varied linearly with log t and had a slope of -7/5. Specimen density therefore varied linearly with $t^{-2/5}$ according to Eq. (1).

$$\rho = \rho_{t=\infty} - \alpha \; t^{-2/5} \tag{1}$$

An empirical expression relating densification rate and porosity can be derived. Differentiating Eq. (1),

$$\frac{d\rho}{dt} = \frac{2 \; \alpha}{5} \; t^{-7/5} \tag{2}$$

substituting Eq. (1) in Eq. (2),

$$\frac{d\rho}{dt} = \frac{2 \; \alpha^{-5/2}}{5} \; \rho_{t=\infty}^{-7/2} \left(\frac{\rho_{t=\infty} - \rho}{\rho_{t=\infty}}\right)^{7/2} \tag{3}$$

and assuming that $\rho_{relative} = \dfrac{\rho}{\rho_{t=\infty}}$ and $1 - \rho_{relative} =$ fractional

porosity[*] yields

$$\frac{d\rho}{dt} = k \ (\text{fractional porosity})^{7/2} \tag{4}$$

where k, the rate constant, is

$$k = \frac{2}{5} \alpha^{-5/2} \ \rho_{t=\infty}^{-7/2} \tag{5}$$

2. <u>Effect of Temperature and Stress</u>. Densities of compacts originally containing 3% LiF pressed at 2250 psi and temperatures between 700 and 1100°C are plotted vs $t^{-2/5}$ in Fig. 1.[**] A portion of each of the curves, except that for 800°C, follows the relationship of Eq. (1) after an initial period. Plotting log k, the rate constant of Eq. (5) determined for the linear portions of the curves, vs 1/T yields an apparent activation energy of 38 kcal/mole.

Effect of variation of stress between 1250 and 4250 psi on densification behavior was determined at 900 and 1100°C for specimens initially containing 3% LiF. During the last 4 hours of compaction, densities were proportional to $t^{-2/5}$. Densification rates, calculated at a density of 99% for each temperature, were directly proportional to stress; data extrapolated to a zero yield stress.

3. <u>Effect of LiF Content</u>. The effect of varying initial LiF content on densification behavior at 900°C and 2250 psi is illustrated in Fig. 2. Each specimen reached a stage of densification where the density

---

* Based on this definition of density during compaction, the actual porosity is inversely related to the volume fraction of the compact that is not occupied by MgO. Density at time equal infinity, $\rho_{t=\infty}$, is associated with the extrapolation of the straight line portion of the curve; thus, fractional porosity as calculated is not a true porosity.

** Like behavior was observed for a specimen pressed at 670°C.

was proportional to $t^{-2/5}$. Specimens containing 5 or more percent

showed almost linear behavior throughout compaction. Specimens contain-

ing 1/2 and 1% initially densified at a high rate followed by a greatly

decreased rate prior to the stage where the $t^{-2/5}$ dependence was followed.

In Fig. 3, the variation of specimen final hot-pressed density is

shown as a function of initial and hot-pressed Li content. Compacts

initially containing 1 or more wt % LiF had approximately equal final Li

contents of about 0.30%, i.e. 1% LiF, and equal densities after pressing.

A specimen initially containing 1/2% LiF had a significantly higher

density but lost no LiF during pressing. The dashed line represents

specimen theoretical densities based on the assumption that all the Li

in the compact after pressing is present as LiF and phases of either

higher or lower density are not present. This calculation does not dis-

tinguish whether the LiF is present as a separate phase or as an ideal

solution with MgO.

Lattice parameters of hot-pressed specimens were used to calculate

the solubility of LiF in MgO with Vegard's law. At 900°C, a LiF solu-

bility in MgO corresponding to 0.075 wt% Li was calculated for the com-

pacts containing 0.30 wt% Li after pressing. Therefore, the bulk of the

LiF does not appear to be in solution. The amount of LiF in solution

decreased with increasing pressing temperature above 900°C. The applica-

tion of stress alone was found to have no effect on the MgO lattice para-

meter.

B. Annealing

Densities of hot-pressed specimens fabricated at temperatures between

830 and 1100°C were in excess of 99%. After annealing at 1300°C for

3 hours in air, specimens had densities in excess of 99.9%, were color-less and had excellent transparency. Densities of the solid phase that volatized during annealing were calculated from volume and compact weight changes during annealing. Values fell between 2.3 and 2.7 gm/cc; the calculated LiF X-ray density is 2.64 gm/cc. The lattice constant of specimens after annealing equalled that of pure MgO.

The rate of weight loss from a specimen was determined thermo-gravimetrically in air at a constant heating rate of 1°/min. If LiF evaporates out of grain boundaries, the evaporating surface area is pro-portional to the amount of LiF present. The instantaneous rate of weight loss measured at a temperature was corrected for loss of evaporating sur-face area by dividing by the weight of the unevaporated LiF. A plot of the log of the corrected rate of weight loss vs 1/T, as shown in Fig. 4, is linear between 830° and 1075°C, yielding a heat of evaporation of 54 kcal/mole at an average temperature of 950°C. Above 1100°C no further weight loss was observed. A heat of 60.5 kcal/mole was calculated for 716°C which agrees well with the value of 58.3 kcal/mole reported by Evseev, et al.[19] for the heat of sublimation of LiF at 716°C. Although this work was not carried out under equilibrium conditions, the close agreement of these values implies that the annealing process above 830°C is controlled by LiF evaporation.

Specimens annealed at 1100°C and below, although becoming trans-parent, developed a pink coloration. In these cases the annealed den-sities were in excess of 99.9% but less than those of specimens annealed at 1300°C. Coloration was retained after annealing 120 hours at 900°C but was lost after reannealing in air for three hours at 1300°C. The

effect was not reversible. Specimens annealed at 900°C in vacuum became transparent and colorless.

C. Deformation with Temperature

Compressive strain vs temperature data shown in Fig. 5 were determined on several specimens at a stress of 750 psi and a heating rate of 250°C/hour using apparatus described by Hulse and Copley.[20] Specimens were cut into right rectangular parallelepipeds with length to width ratios about 1.7.

An annealed specimen exhibited thermal expansion behavior that agrees with Skinner's expansion data for MgO and became opaque when stressed to failure. An unannealed hot-pressed specimen, however, developed a total true strain of about 50%. Its strain i. seen to first deviate from the expansion curve of the annealed specimen at about 630°C with a large increase in the strain rate occurring at about 830°C. The unannealed translucent specimen became optically transparent during the test.

D. Phase Relationships

A number of experiments were performed to determine the phase relationship between MgO and LiF. The eutectic for this system was calculated thermodynamically, on the basis of melting point lowering, to occur at 846°C at a composition of 0.5 wt% MgO-99.5 wt% LiF. Phases other than MgO and LiF were not detected in X-ray analyses of any specimens. However, on the basis of chemical analysis the MgO powder contained cation, hydroxide, and carbonate impurities.

DTA experiments on MgO and LiF powder mixtures showed a small endotherm starting at about 280°C and a larger one at about 830°C. In

mixtures with 20% LiF, slight endothermic activity centered around 550°C was detected. In powders containing no LiF an endothermic reaction occurred between 280 and 350°C. In thermogravimetric studies of the MgO powder, onset of weight loss normally began in this temperature range.

Qualitative diffusion studies were performed on LiF and MgO single crystal couples heated in a closed graphite cell at 800°C for 24 hours. Results obtained on a Material Analysis Co. electron probe indicate that diffusion of Mg into the LiF had taken place with a diffusion zone of about 10μ. It was not possible to measure the diffusion of Li into MgO with this technique.

IV. DISCUSSION

The densification of MgO compacts containing LiF additions can be considered as a three stage process: (I) rearrangement and (II) pressure-flow enhanced liquid phase sintering, both of which occur during hot pressing, and (III) vaporization of the accessory phase, which normally occurs during annealing. During hot pressing, transition zones exist between the successive steps. The extent of the zones depends upon the process parameters.

A. Rearrangement

The initial rapid densification, after load application, is believed to primarily involve a heterogeneous movement of particles under pressure. Compacts sinter away from die walls during heating to the experiment temperature. When the load is applied after temperature stabilization, as in the present experiments, rearrangement involves a lateral flow of material since pressed specimens always filled the dies from

wall to wall. This movement corresponds to the initial rearrangement stage discussed in sintering literature but is enhanced under stress primarily by the lubricating effect of the liquid phase. Rice[1] has found that LiF acts as a lubrication agent between MgO single crystals. Fracturing or localized plastic deformation due to transitory stress concentrations, and solution of MgO by the liquid at points of contact would enhance rearrangement. A quantitative kinetic analysis of this step was not performed. Presintering during heating to experimental temperatures was observed to start at about 280°C. This sintering is due to the onset of hydroxyl decomposition.[21]

B. Pressure-Flow Enhanced Liquid Phase Sintering

Densification during the second stage of hot-pressing is treated as a liquid phase sintering process occurring in grain boundary channels. This stage begins after cessation of major particle rearrangement.

On the basis of electron microscope observations of hot-pressed specimens by Carnall[5] and by Rhodes et al.[4] and lattice parameter measurements in this work, the presence of a lithium fluoride-rich phase on grain boundaries is assumed. Infrared transmission studies indicate that hydroxyl and carbonate ions are associated with this LiF film. Stringer and co-workers[22] have suggested that due to a eutectic reaction between LiF and LiOH, part of the film may be liquid at temperatures as low as 604°C. A complex eutectic reaction between impurities, MgO, and LiF may result in liquid formation at an even lower temperature. The amount of liquid formed by such a multiphase eutectic reaction is expected to be small, since the starting powders had small amounts of impurities; the corresponding endothermic effect would thus be small and difficult to

detect in DTA experiments and could be masked by changes in compact conductivity caused by the onset of sintering. With increasing temperature, the liquid content would be expected to first increase relatively slowly above the multicomponent eutectic temperature and then more rapidly as $846°C$, the calculated MgO-LiF eutectic, is approached; this behavior could account for the endotherms observed at about $550°$ and $830°C$. Due to wetting of MgO, a thin film of liquid covers the particle surfaces including points of contact. Therefore, above $550°C$ sintering would occur in the presence of a liquid phase.

Magnesium oxide redistribution is believed to occur by a solution-precipitation mechanism enhanced by pressure-induced flow. Solution of solid into the liquid at points of contact results in a transient supersaturation and a tendency toward an increase in the volume of the liquid. The applied pressure causes supersaturated liquid to flow out of contact areas with excess MgO precipitating at low energy sites. In normal liquid phase sintering, this pressure contribution is lacking and also densification ceases when all the interstices become filled with liquid. In pressure-flow enhanced liquid phase sintering, densification continues beyond this point since liquid can be forced out of the compact. Due to liquid flow expected MgO concentration gradients due to diffusion do not exist in the liquid.

The rate of densification resulting from flow of liquid out of grain boundary channels should be proportional to the third power of fractional porosity and to the fourth power for a collapsing capillary (see appendix for derivation). These dependencies would be followed whenever a continuous liquid film is maintained around all the grains.

The deviation of the measured porosity dependence of 3.5 from the predicted values may be due to changes in grain size and geometry non-ideality.

Initial LiF content affects the length of time and the range of densities that the $t^{-2/5}$ relationship (stage II) is followed. Compacts initially containing 1/2 (see Fig. 2) and 1% LiF (from which no LiF was lost during pressing), displayed stage II behavior after a long transition region with low densification rates. These low rates may be due to a transitionary region when there is not enough liquid present to maintain the process throughout the compact. The $t^{-2/5}$ relationship is followed at earlier times and lower densities as the initial LiF and the resulting liquid content is increased. At lower temperatures, stage II behavior occurred at lower densities and later times. Here at the time of the load application the particle framework is more open due to less presintering.

The second stage behavior was not observed with compacts pressed at 800°C. Below 830°C the amount of liquid phase depends upon the concentration of carbonates and hydroxides. These are lost by decomposition at elevated temperatures. If enough decomposition occurs, the liquid phase concentration may be reduced to the extent that the pressure enhanced solution-precipitation process becomes inoperative and densification is retarded. From 830 to 1100°C densification followed the $t^{-2/5}$ relationship because of additional liquid formation near the LiF-MgO eutectic temperature. At 1200° and 1300°C, the compacts were porous and densification did not follow the $t^{-2/5}$ relationship. Due to the high vapor pressure of LiF at these temperatures, the compacts were

probably depleted of LiF again resulting in insufficient liquid to sustain the densification process.

On the basis of the proposed mechanism, the measured activation energy of 38 kcal/mole should be that for viscous flow of the LiF-rich liquid. It does not match reported values for the self-diffusion of magnesium and oxygen in MgO single crystals and for normal and pressure sintering of MgO without a LiF additive.

C. Vaporization of Accessory Phase

During annealing, the removal of an essentially uniform LiF-rich film along grain boundaries is controlled by vaporization of LiF from the compact surface. Removal of this phase results in reduction of light scattering at grain boundaries, and a corresponding increase in transparency.

As material evaporates from the specimen surface, the LiF-rich phase is pulled toward the surface by surface tension through grain boundary channels. As a result, the grains at the interior end of the channels are pulled closer together without the formation of pores. Void formation would result in the creation of liquid-vapor interfaces within the compact and an increase in surface-free energy. The process continues until the last of the liquid evaporates from the compact surface.

In hot pressing, due to the relatively tight fit between the plunger and die walls, vaporization of the LiF from the specimen is apparently retarded up to about 1200°C. For specimens pressed at 1000 and 1100°C, the stage II behavior stopped after about 50 minutes of hot pressing. Beyond this point, densities approached the theoretical value. The

center of the specimen pressed at 1100°C was optically transparent while the edges were translucent. These occurrences could constitute a transition period between the flow and the annealing steps.

If densification during annealing is controlled by evaporation, the process should be more rapid in vacuum than in air. In air annealing, a LiF atmosphere would build up near the surface of the specimen that would inhibit LiF loss. It was found that a specimen pressed at 900°C developed much higher transparency when annealed at 900°C in vacuum than in static air or in the die.

D. Deformation with Temperature

The presence of a liquid film on the MgO grain boundaries of hot-pressed specimens, and its effectiveness as an aid to mass transport, is further substantiated by the observed difference in compressive creep behavior of unannealed and annealed specimens. The development of optical transparency and maintenance of grain boundary continuity on straining unannealed specimens in excess of 50% strain can be explained on the basis of a rapid solution-precipitation mechanism resulting in redistribution of MgO during deformation.

In contrast, transparent annealed specimens when strained to failure became opaque. Relatively small strains in the absence of an adequate mechanism for material transport result normally in the creation of cavities at the grain boundaries which lead ultimately to failure of the specimens. Where a liquid phase is not present, maintenance of continuity between grains is normally achieved by plastic deformation. On the basis of the von Mises analysis, polycrystalline MgO must have five active independent slip systems during plastic deformation in order to

maintain grain boundary continuity. This criterion is normally not met by MgO at 1000°C as in this case.[23]

V. SUMMARY

The fabrication of transparent polycrystalline MgO occurs in three stages. During hot pressing, rearrangement of particles and pressure-flow enhanced liquid phase sintering take place. During annealing the remaining liquid is removed by vaporization. The hot pressing steps are separated by a transition zone. At higher temperatures the third stage may begin during hot pressing. The duration of the respective steps is dependent upon process parameters, e.g., LiF concentration, temperature and pressure.

During stage I, heterogeneous rearrangement aided by LiF lubrication is the principal densification mechanism. In stage II, densification proceeds by pressure-enhanced liquid phase sintering where the rate controlling process is viscous flow of the liquid. Application of pressure allows densification to proceed beyond the point where all interstices are filled with liquid. The temperature at which the liquid forms is dependent upon impurities. Transparency is attained during stage III when the liquid forming components are removed by evaporation.

This three stage densification process for fabricating single phase polycrystalline material with the aid of a fugitive phase thus depends upon an additive with the following criteria:

(a) The additive forms a eutectic liquid with the solid and adsorbed impurities and the liquid forms an adhering film on the surface of the solid particles, which is retained during movement of the particles and flow of the liquid;

(b) Further, the additive must have a sufficiently high vapor pressure to allow its removal from the specimen by vaporization at a moderate temperature, and

(c) The solubility of the additive in the solid material must be small at the annealing temperature.

ACKNOWLEDGMENTS

Thanks are extended to T. G. Langdon and D. R. Cropper for helpful discussions and assistance in performing the creep experiment.

Table I. Characterization of MgO Powder

I. Spectrographic analyses before and after pressing, and after annealing.

Impurities	Before pressing, percent	After pressing, percent	After annealing, percent
Si	0.01	0.004	0.007
Al	0.03	0.005	0.003
Li	<0.005	0.2	<0.05
Ca	0.04	0.03	0.02
Fe	0.002	0.002	0.003
Cu	0.0008	0.001	0.0007
Na	0.05(?)	0.05(?)	--
Cr	<0.002	<0.002	<0.002
Mn	<0.001	<0.001	<0.001
Ni	<0.002	<0.002	<0.002
Ba	--	--	--
Sr	--	--	--

Analysis performed by American Spectrographic Laboratories, San Francisco, California.

II. A surface area of 9 ± 2 m^2/gm was determined using a Perkin-Elmo-Shell sorptometer, corresponding to a BET particle diameter of 0.19 μ.

III. Carbon dioxide analysis and weight loss after heating to 1100°C in air indicated the powder contained 0.6 wt % CO_2 and 2.1 wt % H_2O.

APPENDIX

Porosity dependence of the densification rate $(\frac{d\rho}{dt})$ for flow paths behaving as capillaries and channels.

Case I. A flow path with a circular cross section and radius shrinking as liquid is removed from it. According to Poiseuille's equation, the flow rate through the capillary is:

$$\frac{dV}{dt} = \frac{\pi \Delta P\, R^4}{8\, l\eta}$$

where   V = volume of liquid in the channel

η = viscosity of the liquid

ΔP = pressure drop along channel

R = capillary radius

l = capillary length

For a capillary shrinking radially the apparent porosity is proportional to R^2 if the path length remains constant.

$$\therefore \frac{dV}{dt} \propto (\text{Porosity})^2$$

$$\frac{d\rho}{dt} \propto \frac{dV}{dt} \propto (\text{Porosity})^2$$

For a capillary shrinking in only one radial direction (i.e., changing from circular to elliptical cross section) the apparent porosity is proportional to R.

$$\therefore \frac{dV}{dt} \propto (\text{Porosity})^4$$

$$\frac{d\rho}{dt} \propto (\text{Porosity})^4$$

Case II. Paths having a rectangular cross section with the thickness decreasing as liquid is removed. Poiseuille's equation derived for a channel of constant length ℓ, and width a, but variable height χ is

$$\frac{dV}{dt} = \frac{2a}{3} \frac{\Delta P}{\ell\eta} \chi^3$$

porosity $\propto \chi$

$$\therefore \frac{dV}{dt} \propto (\text{Porosity})^3$$

$$\frac{d\rho}{dt} \propto \frac{dV}{dt} \propto (\text{Porosity})^3$$

REFERENCES

1. R. W. Rice, "Production of Transparent MgO at Moderate Temperatures and Pressures," presented at the 64th Annual Meeting of the American Ceramic Society, New York, N. Y., April 30, 1962.

2. M. W. Benecke, N. E. Olson and J. A. Pask, "Effect of LiF on Hot-Pressing of MgO," J. Am. Ceram. Soc., 50 (7) 365-368 (1967).

3. C. Herring, "Diffusional Viscosity of a Polycrystalline Solid," J. Appl. Phys., 21 (5) 437-445 (1950).

4. W. Rhodes, D. Sellers, and T. Vasilos, "Development and Evaluation of Transparent Magnesium Oxide," Avco Corp. AMRA CR 67-01 (F) Feb. 1967.

5. E. Carnall, Jr., "The Densification of MgO in the Presence of a Liquid Phase," Mat. Res. Bull. Vol 2, 1075-1086 (1967).

6. E. D. Kingery, "Densification During Sintering in the Presence of a Liquid Phase. I. Theory," J. Appl. Phys., 30 (3) 301-306 (1959).

7. G. D. Miles, R. A. J. Sambell, J. Rutherford and G. W. Stephenson, "Fabrication of Fully Dense Transparent Polycrystalline Magnesia," Trans. Brit. Ceram. Soc., 66 (7) 319-335 (1967).

8. T. Vasilos and R. M. Spriggs, "Pressure Sintering: Mechanisms and Microstructures for Alumina and Magnesia," J. Am. Ceram. Soc., 46 (10) 493-496 (1963).

9. R. L. Coble, "Sintering Crystalline Solids. I. Intermediate and Final Stage Models," J. Appl. Phys., 32 (5) 787-792 (1961).

10. R. L. Coble and T. K. Gupta, "The Intermediate State of Sintering: Models and Experimental Results," presented at the 67th Annual Meeting, American Ceramic Society, Philadelphia, Pa., May 3, 1965.

11. R. A. Brown, "Sintering in Very Pure Magnesium Oxide and Magnesium Oxide Containing Vanadium," Bull. Am. Ceram. Soc., 44 (6) 483-487 (1965).

12. R. Lindner and G. D. Parfitt, "Diffusion of Radioactive Magnesium Oxide Crystals,: J. Chem. Phys. 26 (1) 182-185 (1957).

13. Y. Oishi and W. D. Kingery, "Oxygen Diffusion in Periclase Crystals," J. Chem. Phys., 33 (3) 905-906 (1960).

14. P. F. Eastman and I. B. Cutler, "Effect of Water Vapor on Initial Sintering of Magnesia, "J. Am. Ceram. Soc., 49 (10) 526-530 (1966).

15. W. D. Scott and J. A. Pask, "Deformation and Fracture of Poly-crystalline Lithium Fluoride," J. Am. Ceram. Soc., 46 (6) 284-293 (1963).

16. B. J. Skinner, "The Thermal Expansion of Thoria, Periclase and Diamond," Amer. Min., 42 (1 and 2) 39-55 (1957).

17. R. C. Rossi and R. M. Fulrath, "Final Stage Densification in Vacuum Hot-Pressing of Alumina," J. Am. Ceram. Soc., 48 (11) 558-565 (1965).

18. G. M. Fryer, "Hot-Pressing of Alumina, A Treatment of Final Densi-fication," Trans. Brit. Ceram. Soc., 66 (3) 127-134 (1967).

19. A. M. Evseev, G. V. Pozharaskaya, A. N. Nesmeyanov and Ya. I. Gerasimov, "Vapour Pressure of Lithium Fluoride," Russ. J. Inorg. Chem. (English Translation) 4 (10) 997-998 (1959).

20. C. O. Hulse and S. M. Copley, "High-Temperature Compressive Deforma-tion Equipment," Am. Ceram. Soc. Bull, 45 (5) 530-534 (1966).

21. P. W. Sunderland and A. C. D. Chaklader, "Deformation During De-hydroxylation of Hydroxide," Mat. Res. Bull. 2, 1111-1118 (1967).

22. R. W. Stringer, C. E. Warble and L. S. Williams, "Phenomenological Observations in Decomposition and Sintering Reactions," presented at International Symposium on Ceramics, Alfred University, Alfred, N. Y., June 1967.

23. S. M. Copley and J. A. Pask, "Deformation of Polycrystalline MgO at Elevated Temperatures," J. Am. Ceram. Soc., v. 48, pp. 636-642, Dec. 1965.
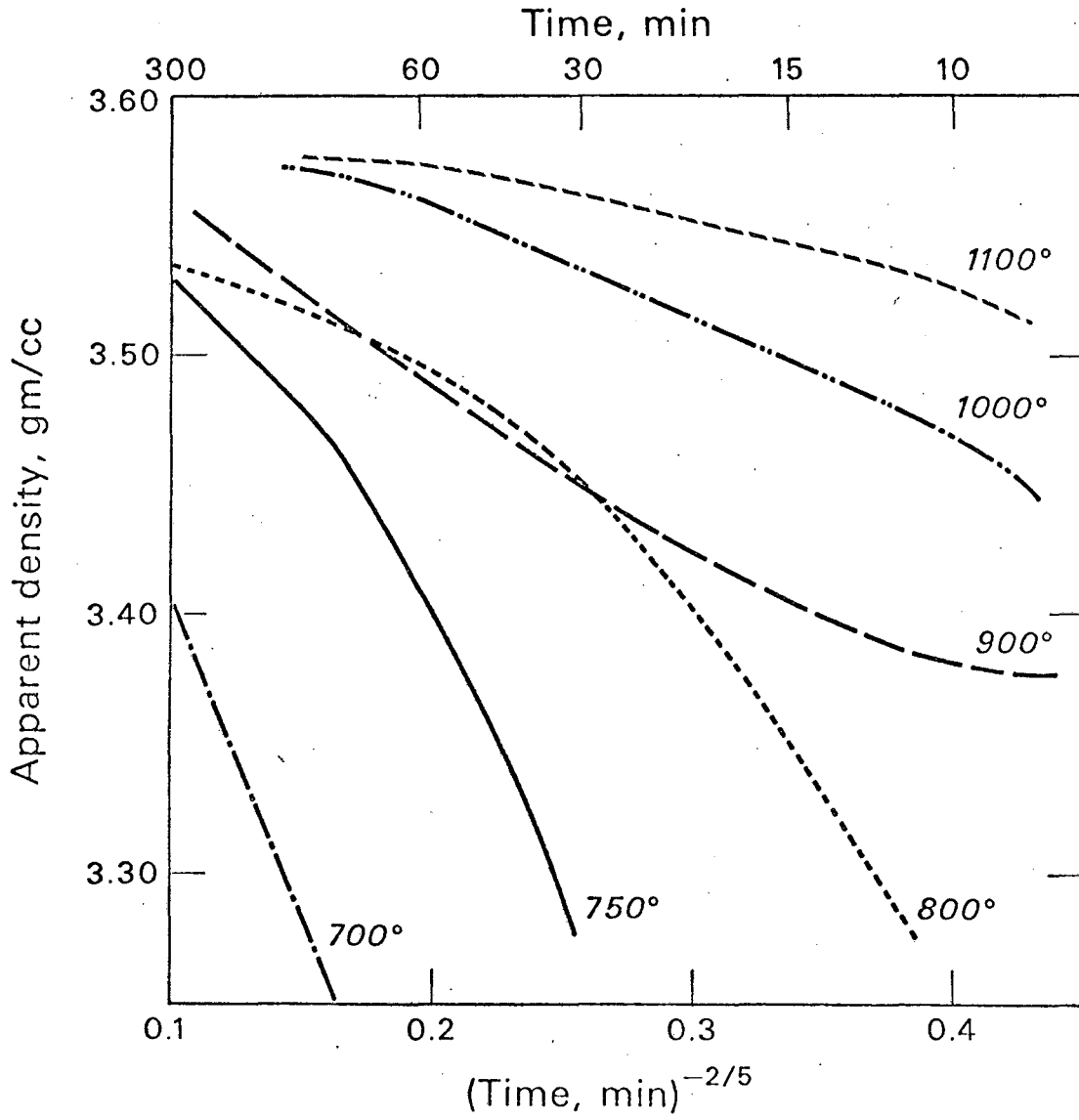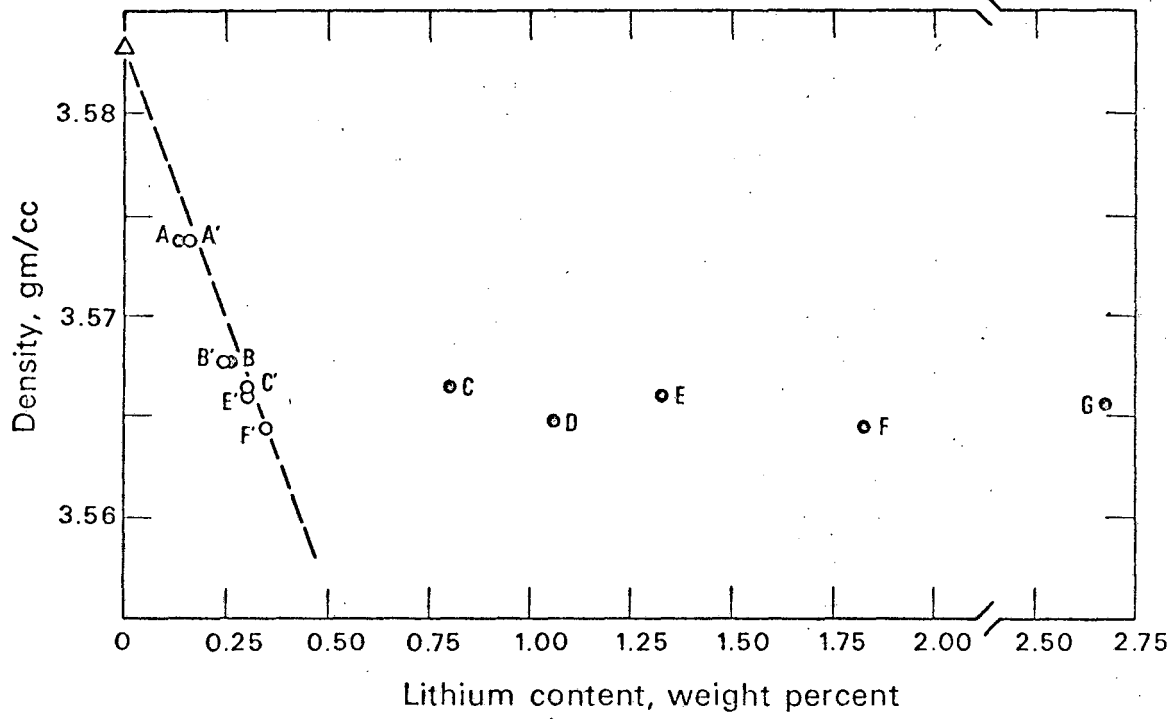
Fig. 1 Effect of temperature on densification
of specimens initially containing 3%
LiF pressed at 2250 psi.
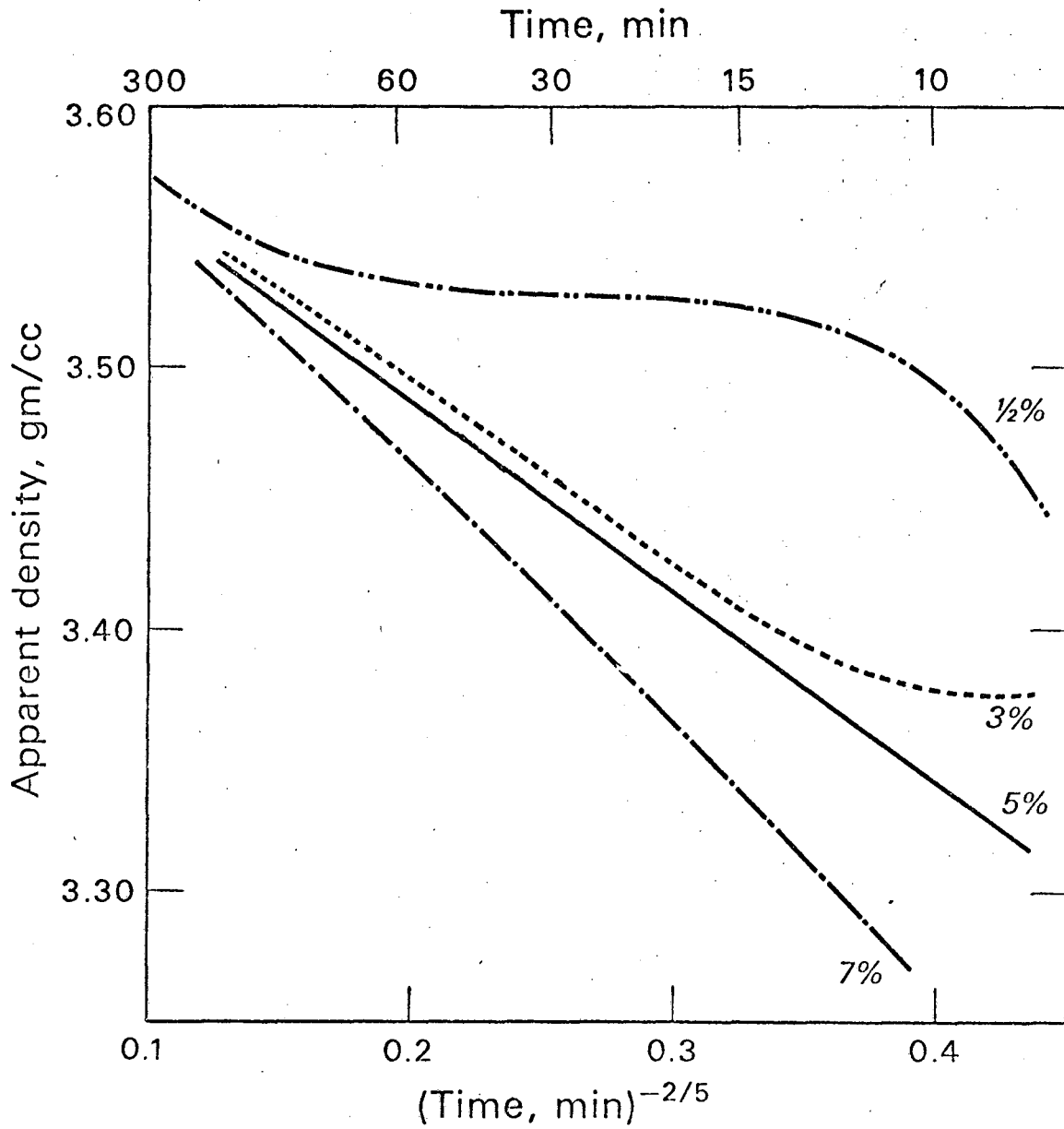
XBL 6712-1972

Fig. 2 Effect of initial LiF content on densification of specimens pressed at 900° C/2250 psi.

XBL 6712-1976

XBL 6712-1982

Fig. 3 Variation of specimen final density as a function of initial and as hot-pressed lithium content

● Li content before pressing, O Li content after pressing, △ theoretical density of MgO
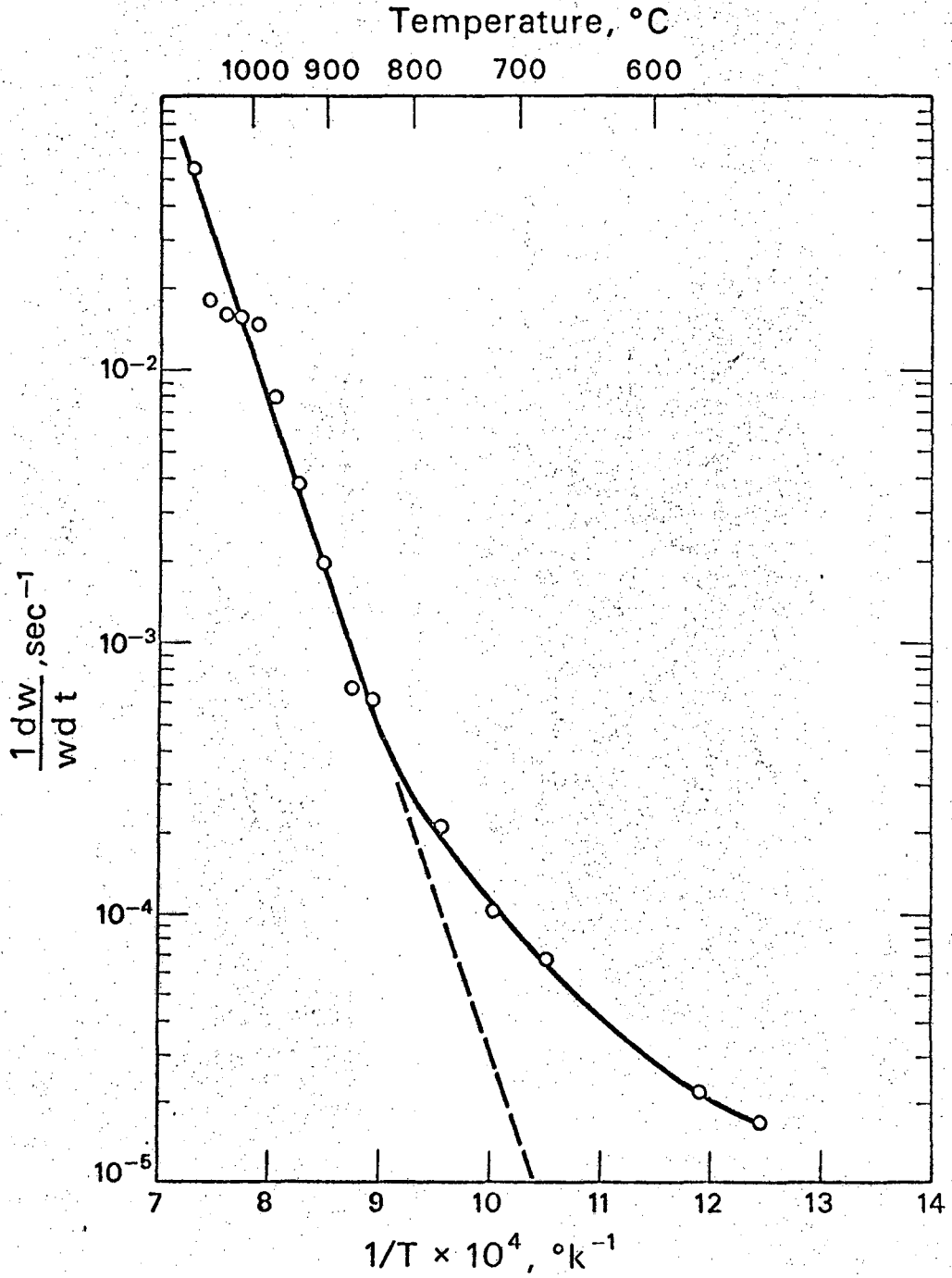
Fig. 4 Rate of weight loss from a hot-pressed specimen as a function of temperature.
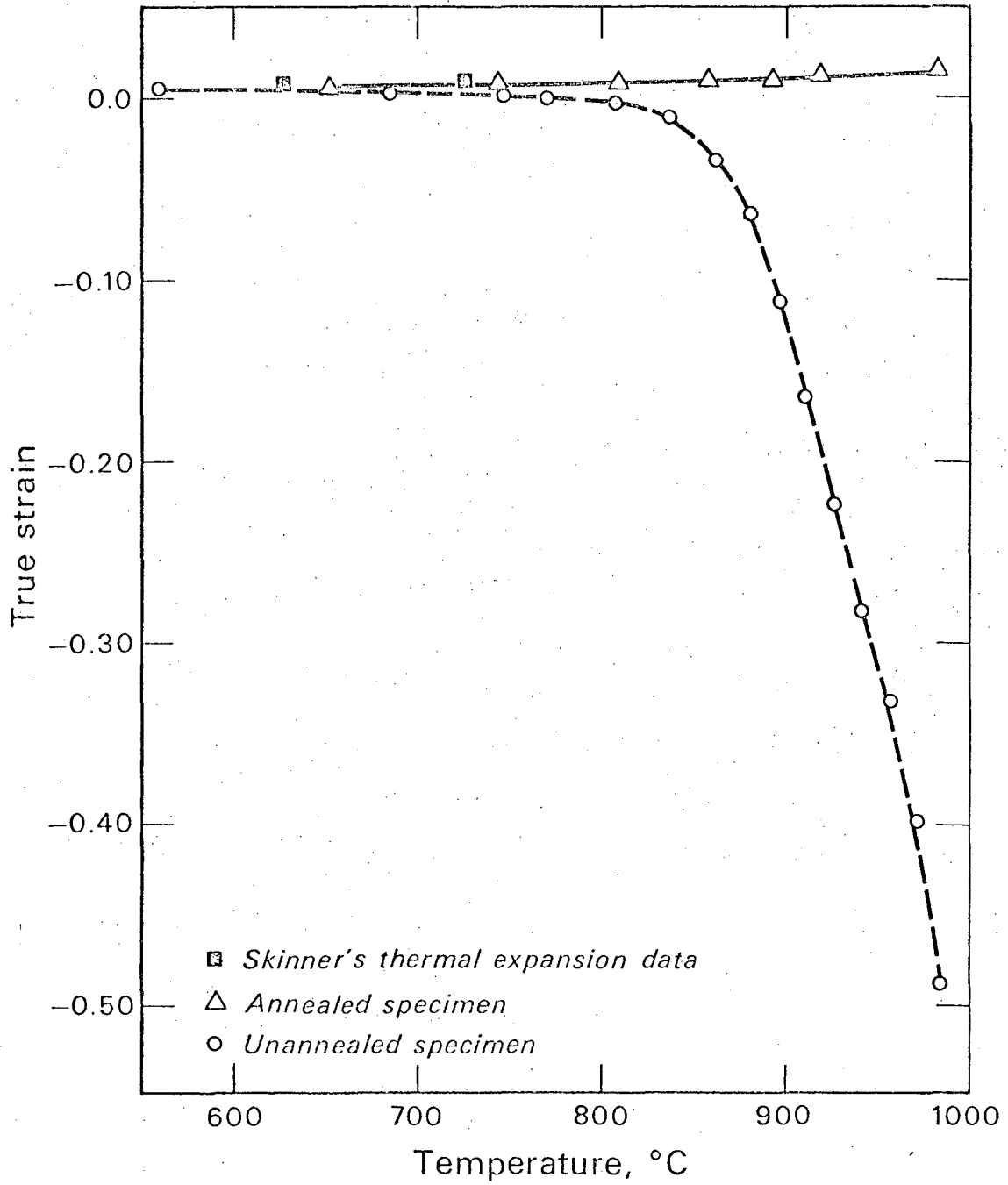
XBL 6712-1979

XBL 6712-1984

Fig. 5 True strain on heating of annealed and unannealed specimens under a stress
of 750 psi.